

# Using MoC for SERN Design: Theory and Programming Methodology

Neelay Doshi \*

**This report presents a brief overview of SERN design for hypersonic vehicles. An in-house code was developed using method of characteristic. The results were validated against both inviscid and viscous CFD.**

## I. Nomenclature

$M$	=	Mach number
$P$	=	pressure
$T$	=	temperature
$u$	=	$x$ component of velocity
$v$	=	$y$ component of velocity
$V$	=	velocity magnitude
$\gamma$	=	specific heat ratio
$\nu$	=	Prandtl-Meyer function
$\phi$	=	velocity potential function
$\rho$	=	density
$\theta$	=	slope of streamline
Subscript		
0	=	stagnation condition or inlet
$char$	=	characteristic line
$e$	=	exit

---

\*M.Tech Student, Department of Aerospace Engineering, IIT Kharagpur.

## II. Introduction

Hypersonic vehicle nozzles which are responsible for generating the thrust are generally fused with the vehicle aft-body, thus influencing the thrust efficiency and vehicle stability. Single expansion ramp nozzles (SERN) are the subject of analysis of this work. Nozzle's function is to accelerate the heated air from the combustor to produce thrust in a scramjet engine, transforming the flow internal energy into kinetic energy. The nozzle design is critical to obtain the necessary thrust to accelerate an aerospace vehicle. Since in a scramjet, the flow is supersonic through-out its flow through the engine, the flow velocity at the nozzle inlet is also supersonic ( $M > 1$ ) and so the code developed in this study is applicable only for inlet Mach number greater than 1 ( $M_0 > 1$ ).

## III. Theory of Method of Characteristics

(**Note:** This section presents a brief overview of the theory governing supersonic flows, as described in *Fundamentals of Aerodynamics* [1]. Please refer to it for a detailed explanation.)

Let us assume an inviscid, compressible and irrotational flow through a nozzle. As the flow occurs at high velocity, its residence time is short, we can assume the heat transfer to or from the wall is negligible. We can also neglect the frictional losses and thus assume the flow to be isentropic. The governing conservation equations for such a flow in two dimension are given below:

*Mass Conservation:*

$$\frac{\partial(\rho u)}{\partial x} + \frac{\partial(\rho v)}{\partial y} = 0 \quad (1)$$

*Momentum Conservation:*

$$\rho V dV = -dP \quad (2)$$

*Energy Conservation:*

$$h + \frac{V^2}{2} = h_0 \quad (3)$$

As the flow is irrotational, a *velocity potential*  $\phi$  exists and thus the velocity component can be defined as:  $u = \partial\phi/\partial x$  and  $v = \partial\phi/\partial y$ . These expressions can then be substituted into the continuity equation for a two dimensional flow to obtain the following relation:

$$\rho \left( \frac{\partial^2 \phi}{\partial x^2} + \frac{\partial^2 \phi}{\partial y^2} \right) + \frac{\partial \phi}{\partial x} \frac{\partial \rho}{\partial x} + \frac{\partial \phi}{\partial y} \frac{\partial \rho}{\partial y} = 0 \quad (4)$$

As we wish to obtain the equation in terms of  $\phi$ , we must eliminate  $\rho$  from the above equation. To do so, we employ

the Eq. (2) which is the Euler's equation for momentum conservation. As the flow is assumed to be isentropic, we can relate the change in pressure to the change in density as:  $a^2 = (\partial P / \partial \rho)_s$ , where  $a$  is the speed of sound. The Euler's equation can then be re-written in terms of  $\phi$ ,  $\rho$  and  $a$  as:

$$d\rho = -\frac{\rho}{2a^2} d \left[ \left( \frac{\partial \phi}{\partial x} \right)^2 + \left( \frac{\partial \phi}{\partial y} \right)^2 \right] \quad (5)$$

The above equation is the total derivative of  $\rho$  which upon partial differentiation w.r.t  $x$  and  $y$  can be plugged into the Eq. 4 to yield the following equation:

$$\left[ 1 - \frac{1}{a^2} \left( \frac{\partial \phi}{\partial x} \right)^2 \right] \frac{\partial^2 \phi}{\partial x^2} + \left[ 1 - \frac{1}{a^2} \left( \frac{\partial \phi}{\partial y} \right)^2 \right] \frac{\partial^2 \phi}{\partial y^2} - \frac{2}{a^2} \left( \frac{\partial \phi}{\partial x} \right) \left( \frac{\partial \phi}{\partial y} \right) \frac{\partial^2 \phi}{\partial x \partial y} = 0 \quad (6)$$

Further, we can employ the energy conservation equation to obtain the expression for speed of sound  $a$  in terms of  $\phi$  and stagnation speed of sound  $a_0$  as follows:

$$a^2 = a_0^2 - \frac{\gamma - 1}{2} \left[ \left( \frac{\partial \phi}{\partial x} \right)^2 + \left( \frac{\partial \phi}{\partial y} \right)^2 \right] \quad (7)$$

Eq. 6 is known as the *velocity potential equation*. Note that the three conservation equations of mass, momentum and energy, which formed a system of partial differential equations, have now been clubbed into a single partial differential equation in terms of velocity potential  $\phi$ . Thus if we have the expression for  $\phi$ , we may obtain all the flow properties:  $u$ ,  $v$ ,  $\rho$ ,  $P$  and  $T$ , because the flow is assumed to be isentropic and thus the stagnation properties:  $\rho_0$ ,  $P_0$  and  $T_0$  are constant throughout the flow field. But this equation is nonlinear and thus needs to be solved numerically. Nevertheless, let us see if we can further simplify this equation for some specific situation.

Let us define "*characteristic lines*" in a two dimension plane as the lines along which the derivatives of the flow field variables are indeterminate and across which they may be discontinuous. For a supersonic flow, if we try to solve Eq. 6 for  $\partial^2 \phi / \partial x \partial y$ , along with the total derivative of  $u$  and  $v$  in terms of  $\phi$ , using Cramer's rule, we find that derivatives of the flow will be indeterminate along the line having the following slope:

$$\left( 1 - \frac{u^2}{a^2} \right) \left( \frac{dy}{dx} \right)_{char}^2 + \frac{2uv}{a^2} \left( \frac{dy}{dx} \right)_{char} + \left( 1 - \frac{v^2}{a^2} \right) = 0 \quad (8)$$

In the above equation,  $(dy/dx)_{char}$  is the slope of the characteristic lines. We can substitute  $u = V \cos \theta$ ,  $v = V \sin \theta$  and

$V^2/a^2 = M^2 = 1/\sin^2\mu$ , to obtain the following reduced form of the slope:

$$\left(\frac{dy}{dx}\right)_{char} = \tan(\theta \mp \mu) \quad (9)$$

Eq (9) tells us that the characteristic lines are inclined at an angle  $\mu$  above and below the streamline. Note that because these lines are inclined at an angle  $\mu$ , the characteristic lines are indeed Mach wave. The line inclined at  $(\theta + \mu)$  is denoted by  $C_+$ , and is called the *left running characteristic*. While the line inclined at  $(\theta - \mu)$  is denoted by  $C_-$ , and is called the *right running characteristic*. Fig. 1 helps visualize the aforementioned description.

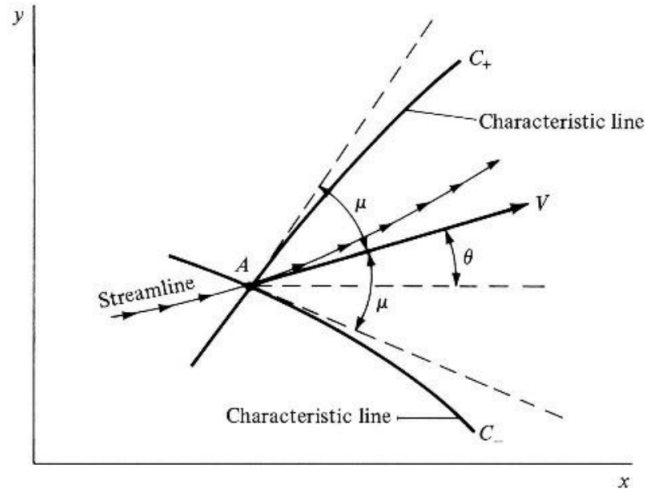


**Fig. 1 Left and right running characteristic lines through point A. [1]**

The indeterminacy of  $(\partial^2\phi/\partial x\partial y)$  yield another relation:

$$\frac{dv}{dx} = \frac{-(1 - u^2/a^2)}{1 - v^2/a^2} \left(\frac{dy}{dx}\right)_{char} \quad (10)$$

Upon substituting the value of  $(dy/dx)_{char}$  into the above equation and doing some algebraic manipulation we obtain the following result:

$$d\theta = \mp \sqrt{M^2 - 1} \frac{dv}{v} \quad (11)$$

$$\nu(M) = \sqrt{\frac{\gamma+1}{\gamma-1}} \cdot \arctan \sqrt{\frac{\gamma-1}{\gamma+1} (M^2 - 1)} - \arctan \sqrt{M^2 - 1} \quad (12)$$

Eq (9) are called the *compatibility equation* while Eq (11) are know as the *compatibility relations*, which hold only along the characteristic lines. Upon integration of Eq (11), the RHS yields the Prandtl-Meyer function  $\nu(M)$  Eq. (12)

and is written as follows:

$$\begin{array}{l} \theta + \nu(m) = K_- = \text{const} \\ \theta - \nu(m) = K_+ = \text{const} \end{array} \quad (13)$$

Thus, in summary, we have managed to convert the the conservation equation, which were a coupled system of PDEs, first into a single PDE in terms of  $\phi$ , given by Eq (6), which was valid throughout the flow field. Then, using the indeterminacy criterion, we converted it to an ODE, given by Eq (9) and Eq (11), which are valid only along the *characteristic lines*. Upon integration, we finally obtain Eq (13), which states that the sum of the flow angle  $\theta$  and the Prandtl-Meyer function  $\nu$ , remain constant along a characteristic line. The constant  $K_-$  and  $K_+$  correspond to the characteristic lines  $C_-$  and  $C_+$  respectively.

#### IV. Methodology for Programming

Consider the intersection of two characteristic lines passing through point 1 and 2 at point 3 as show in Fig 2. The line passing through point 1 and 2 are the left and right running characteristic lines respectively. From the compatibility relation derived in the previous section, we know that the sum/difference of the flow angle  $\theta$  and Prandtl-Meyer function  $\nu$  remains constant along a characteristic line. Thus,  $(K_-)_3 = (K_-)_1$  and  $(K_+)_3 = (K_+)_2$ . We can then obtain the flow angle  $\theta$  and Prandtl-Meyer function  $\nu$  at node 3 as:

$$\begin{aligned} \theta_3 &= \frac{(K_-)_3 + (K_+)_3}{2} \\ \nu_3 &= \frac{(K_-)_3 - (K_+)_3}{2} \end{aligned} \quad (14)$$

For the wall boundary condition as shown in Fig 2, if the slope of the wall  $\theta_5$  is given, then we can obtain the the flow properties at point 5 from the know proprieties of flow at point 4 as follows:

$$\begin{aligned} (K_-)_4 &= (K_-)_5 \\ \theta_4 + \nu_4 &= \theta_5 + \nu_5 \end{aligned} \quad (15)$$



**Fig. 2 a.) Calculation of flow conditions at point 3 from the known flow properties at points 1 and 2.**  
**b.) Calculation of flow conditions at point 5 from the know flow properties at point 4 and slope point 5 [1]**

This is all quite well and good, but applying this seemingly simple Eq (13) and Eq (15) is a bit tricky. For simplicity, consider Fig 3, which a schematic of a nozzle designed with only four characteristic lines for ease of visualization. The points of intersection of the characteristic lines have been numbered. The origin of the expansion fan has been numbered 0. We see a total of 14 points (excluding the origin of expansion-fan). To be able to compute and plot each of the characteristic lines and obtain the data ( $P$ ,  $T$ ,  $\rho$ ...) at each node with ease, it is imperative to organise the calculation of  $M$ ,  $\theta$  and  $\nu$  at each node.

To do so, let us relabel the MoC schematic in Fig 3. For ease of accessing various nodes and plotting the characteristic

lines, we will identify each of the characteristic lines separately. As we have four characteristic lines, we can label each one as such: 1, 2, 3 and 4. The origin of all the characteristic lines is the same and hence it is redundant to include it in our data set for each of the lines. Thus the first node of the first characteristic line would be point 1 on the base of the nozzle. The second, third and fourth nodes would be as marked in Fig 3. We can identify each of these nodes as  $a_{ij}$ , where  $i$  represents the characteristic line while the subscript  $j$  identifies the node location along the  $i^{th}$  characteristic line. Thus, nodes (1, 2, 3 and 4) in Fig 3 are relabeled as ( $a_{11}$ ,  $a_{12}$ ,  $a_{13}$ ,  $a_{14}$ ) in the left image in Fig 4. Similarly, the second characteristic line and its nodes can be identified as ( $a_{21}$ ,  $a_{22}$ ,  $a_{23}$ ,  $a_{24}$ ) as shown in the right image in Fig 4. Similar labeling can be done for characteristic line 3 and 4.

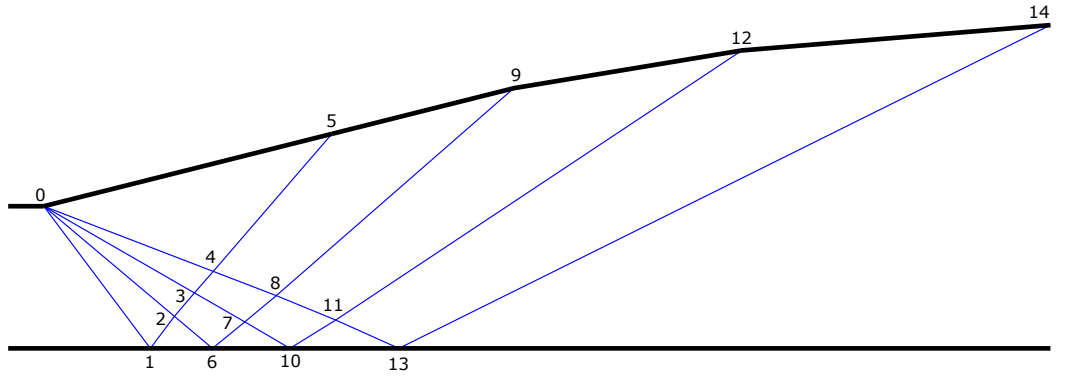


**Fig. 3** Simplified schematic of SERN contour design using MoC with four characteristic lines.

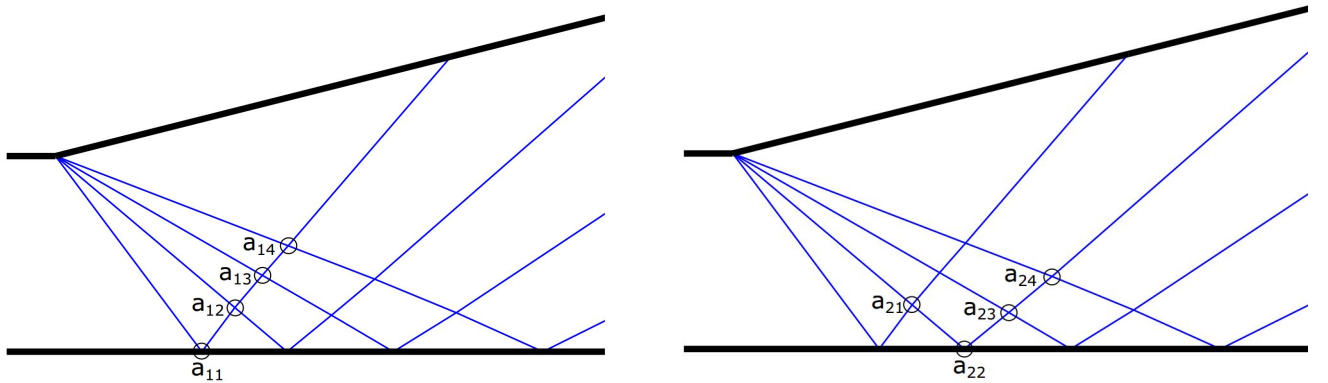


**Fig. 4** Schematic of the *matrix form* of labeling for identifying the intersection points of each characteristic line.

This form of labeling leads to the generation of some symmetric patterns which helps simplify the programming procedure. Let us explore this. Notice that we have four characteristic lines and 4 intersection points for each line. Thus,

we will have a total of  $4 \times 4 = 16$  labels/markers which can be organised into a matrix form as shown in Eq. 16. This also implies that for  $N$  number of characteristic lines we will simply require an  $N \times N$  matrix, wherein the  $i^{th}$  row of the matrix corresponds to the  $i^{th}$  characteristic line. Also, notice that this matrix is symmetric, the node  $j^{th}$  node along the characteristic line  $i$  is the same as the  $i^{th}$  node along the characteristic line  $j$ , thus:  $a_{ij} = a_{ji}$ .

$$[a] = \begin{bmatrix} a_{11} & a_{12} & a_{13} & a_{14} \\ a_{21} & a_{22} & a_{23} & a_{24} \\ a_{31} & a_{32} & a_{33} & a_{34} \\ a_{41} & a_{42} & a_{43} & a_{44} \end{bmatrix} \quad (16)$$

Moreover, notice that each of the diagonal elements  $a_{ii}$  is located on the bottom wall of the nozzle. For the nozzle schematic shown in Fig 3, the characteristic lines are right running  $C_-$  when they originate at point 0, which upon reflection from the bottom wall, become left running  $C_+$  characteristic lines. The constant  $K_{+/-}$  along each of the characteristic lines can be written in the form shown in the LHS of Eq 17. Whats more is that because the flow at the wall must be parallel to the wall, the characteristic constant  $K$  of any of the characteristic lines will simply switch sign after being reflected off the wall. Thus, the matrix for the characteristic constant  $K$  is further simplified to the RHS of Eq 17.

$$[K] = \begin{bmatrix} K_{11+} & K_{12+} & K_{13+} & K_{14+} \\ K_{21-} & K_{22+} & K_{23+} & K_{24+} \\ K_{31-} & K_{32-} & K_{33+} & K_{34+} \\ K_{41-} & K_{42-} & K_{43-} & K_{44+} \end{bmatrix} \Rightarrow \begin{bmatrix} -K_1 & -K_1 & -K_1 & -K_1 \\ K_2 & -K_2 & -K_2 & -K_2 \\ K_3 & K_3 & -K_3 & -K_3 \\ K_4 & K_4 & K_4 & -K_4 \end{bmatrix} \quad (17)$$

In the above matrix,  $K_i$  represents the characteristic constant of the  $i^{th}$  line. To compute this, we require the value of  $\nu_0$  and  $\theta_i$  at the origin of the expansion-fan. For a given inlet Mach number  $M_0$  and desired exit Mach number  $M_e$ , the corresponding value of Prandtl-Meyer function  $\nu_0$  and  $\nu_e$  can be obtained from the Eq 12. The total angle by which the flow would have to turn would then be given as:  $\theta_{total} = \nu_e - \nu_0$ . Thus the angle at the expansion corner (point 0) must be half of the  $\theta_{total}$  as shown below:

$$\theta_{turn} = \frac{\theta_{total}}{2} = \frac{\nu_e - \nu_0}{2} \quad (18)$$

Now for  $N$  number of characteristic lines, the flow turns by an angle  $d\theta = \theta_{turn}/(N - 1)$  across each characteristic line, while the value of the Prandtl-Meyer function after the  $i^{th}$  characteristic line would simply be the sum of the turning angle  $\theta_i$  and the inlet Prandtl-Meyer function  $\nu_0$  as shown below:



$$\begin{aligned}
\theta_i &= \theta_{i-1} + d\theta \\
\nu_i &= \theta_i + \nu_0 \\
K_i &= \theta_i + \nu_i
\end{aligned}
\tag{19}$$

**Note:** The above relation does not hold for  $i = 1$ . In the approach adopted in this study, the first characteristic line corresponds to the Mach wave of the incoming supersonic flow at the inlet, whose Mach number is already known.

The matrix for the flow angles ( $\theta$ ) at each node is also a symmetric matrix wherein the diagonal elements are zero as they represent the nodes at the nozzle lower wall. It can be computed easily by using the simple expression shown below:

$$[\theta] = \frac{\theta_{turn}}{(N-1)} \times \begin{bmatrix} 0 & 1 & 2 & 3 \\ 1 & 0 & 1 & 2 \\ 2 & 1 & 0 & 1 \\ 3 & 2 & 1 & 0 \end{bmatrix}$$

Once the  $K$  and  $\theta$  matrix are computed, we can easily compute the  $\nu$  matrix using the relation given in Eq (19). Thereafter, we can use secant method to obtain the Mach number at each node by solving Eq (12) iterative. Next, the slope of each of the characteristic lines is simply:  $dy/dx = \theta \pm \nu$ , as they are Mach waves. Thus, we have all the necessary parameter for plotting the nozzle contour and obtaining the flow properties such as  $P$ ,  $T$ ,  $\rho$  at each node.

**Note:** The  $\theta$ ,  $\nu$  and  $M$  matrices are all beautifully symmetric. Meaning, one needs to run a for-loop for only the upper triangle of the matrices, thus saving computational time.

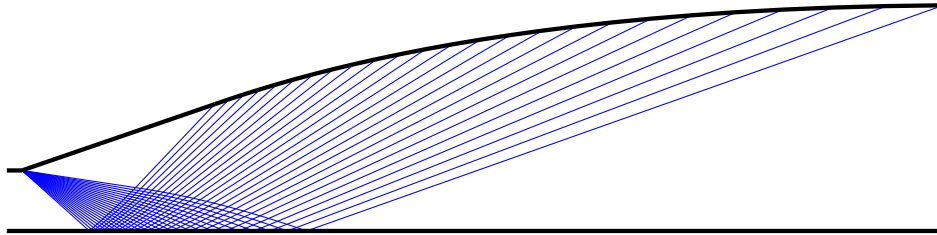


**Fig. 5** SERN contour obtained from MoC code for 25 characteristic lines.

## V. Validation and Results of MoC Code

### A. Theoretical Design

To validate the MoC code, a generic scramjet combustion chamber exit conditions have been chosen as the inlet conditions for SERN as shown in Table 1. The scramjet is assumed to be flying at Mach 6 at an altitude of 30 *km*, which would correspond to an ambient pressure and temperature of 1000 *Pa* and 225 *K* respectively. Assuming the specific heat ratio  $\gamma = 1.4$ , this corresponds to a flight velocity of  $V \approx 1800$  *m/s*. Thus, for the inlet conditions mentioned in Table 1, a SERN designed for an exit Mach number  $M_e = 3$  would give an exit pressure and velocity of approximately 1935 *m/s* and 0.125 *bar* respectively, which are greater than the ambient pressure and flight velocity, and hence would yield positive thrust.

**Table 1** Inlet parameters for CFD simulation of a generic SERN and the theoretical exit parameters.

Parameters	Inlet	Outlet
$M$	1.5	3
$T$	2000 K	1035 K
$P$	1.25 bar	0.125 bar
$T_0$	2900 K	2900 K
$P_0$	4.588 bar	4.588 bar
$a$	896 m/s	645 m/s
$V$	1345 m/s	1935 m/s

$$\frac{A_e}{A^*} = \frac{1}{M} \left( \frac{2 + (\gamma - 1) \cdot M^2}{\gamma + 1} \right)^{\frac{\gamma+1}{2(\gamma-1)}} \quad (20)$$

In a scramjet, the flow is supersonic throughout the engine and thus the nozzle inlet mach number is greater than unity (as shown in Table 1). The ratio of the nozzle exit area  $A_e$  to the throat area ( $A^*$ ) is given by Eq. (20), for an isentropic flow, wherein the Mach number at the nozzle throat is unity. Thus using Eq. (20) we obtained the theoretical inlet to exit area-ratio to be 3.60032 for our SERN, as shown below:

$$\frac{A_e}{A_i} = \frac{A_3}{A_{1.5}} = \frac{A^*}{A_{1.5}} \times \frac{A_3}{A^*} = \frac{1}{1.17616} \times 4.23456 = 3.60032 \quad (21)$$

### B. MoC Design

The first step of validation of our MoC code is to compare the theoretical area-ratio, given by Eq. (21), with that obtained from MoC. Table 2 shows the nozzle area-ratio as obtained from MoC for various number of characteristic lines and the corresponding run-time of the code. Upon running the code for 1000 characteristic lines, the area-ratio was 3.6033, which is  $\approx 0.1\%$  off from the theoretically computed value of 3.60032. Thus, the nozzle contour obtained by using 1000 characteristic lines has been used for mesh generation and CFD simulation.

**Table 2** The exit to inlet area-ratio of SERN as obtained from MoC code for varying number of characteristic lines and the corresponding run time of the code.

No: of Characteristic Lines	Area Ratio	Code Run Time
25	3.7296	0.079 s
50	3.6623	0.082 s
100	3.6307	0.134 s
250	3.6123	0.439 s
500	3.6063	1.432 s
1000	3.6033	4.808 s

### C. Mesh Generation

Fig 6 shows the mesh generated using the nozzle contour coordinates obtained from the MoC code. The right image in Fig 6 shows the magnified view of the top left corner of the nozzle. The mesh has quadrilateral elements (structured mesh) and is generated in ICEM-CFD. The nozzle inlet and exit height are  $100\text{mm}$  and  $360.33\text{mm}$  respectively. The total length of the nozzle is  $1.486\text{m}$ . The first element height near the wall is  $1\mu\text{m}$ , which corresponds to an approximate  $Y+$  value of unity. The growth rate of element normal to the wall is 1.2.

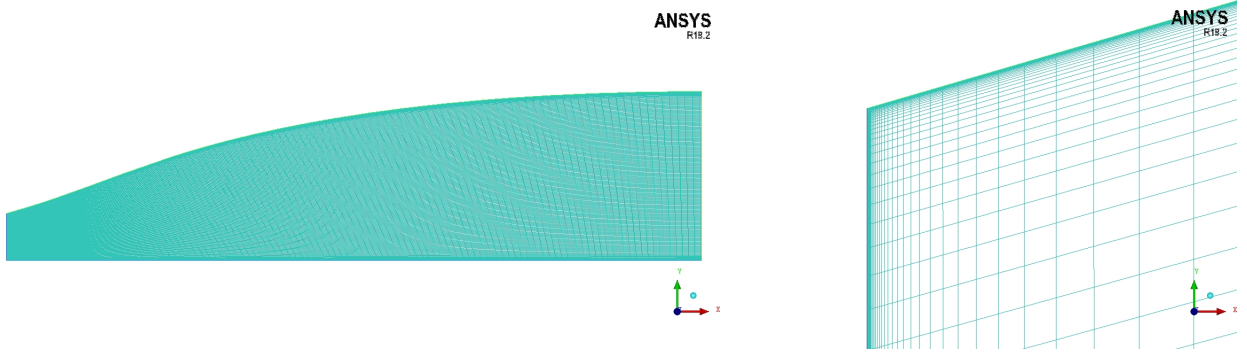


**Fig. 6** Mesh of SERN for viscous CFD

### D. CFD Simulation

Inviscid and viscous simulations have been conducted in ANSYS Fluent to validate the MoC code developed. Fig 7 and 8 shows the velocity and pressure profile of the viscous simulation. The boundary layer is clearly visible in Fig 7. The exit velocity is slightly less than the theoretical value given in Table 1, which is to be expected on account of viscosity. Consequently, the exit pressure is larger than the theoretical value. The consequence of these deviation are discussed in the next subsection.

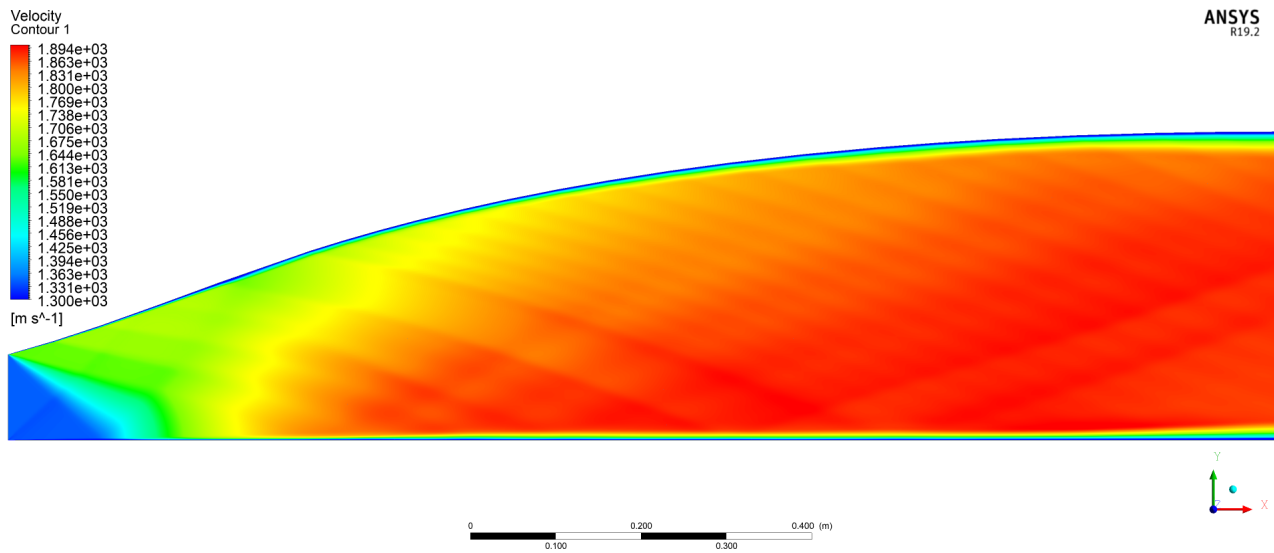


**Fig. 7 Velocity profile of SERN from viscous CFD**

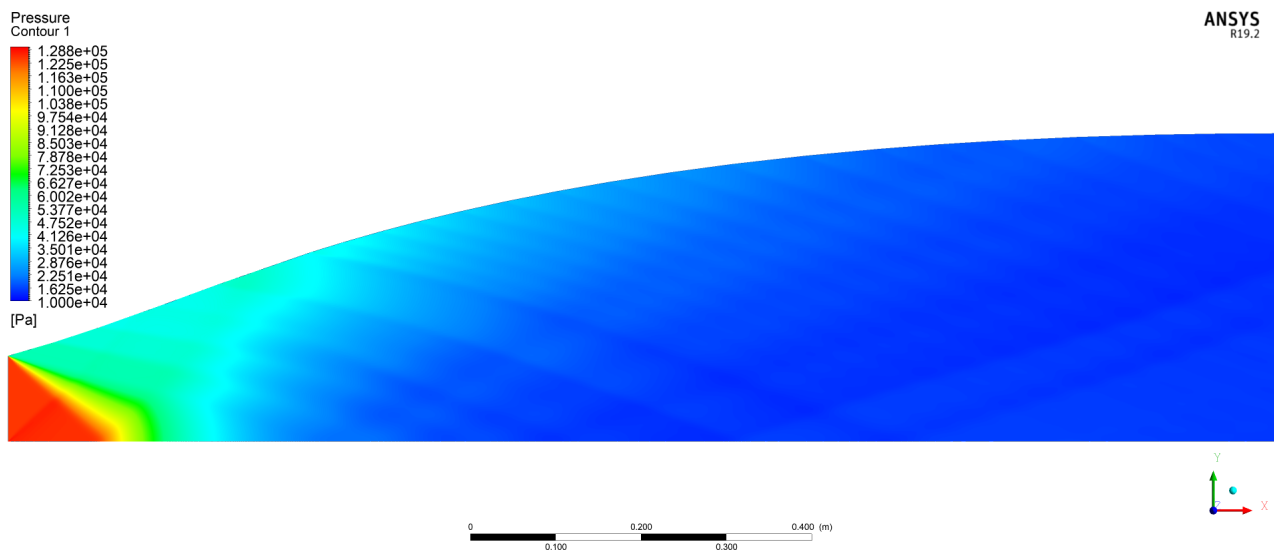


**Fig. 8 Pressure profile of SERN from viscous CFD**

### E. Comparison of MoC with CFD Results

The primary motive for developing the MoC code for SERN design is to obtain the pressure profile over the nozzle contour so as to compute the thrust and lift (force in  $x$  and  $y$  direction respectively) generated by the nozzle within a quick turnaround time, with decent accuracy. As the Mach number is known at every grid point in the MoC code, we can obtain the corresponding static pressure  $P$  using the simple gasdynamic relation:

$$\frac{P_0}{P} = \left[ 1 + \left( \frac{\gamma - 1}{2} \right) M^2 \right]^{\frac{\gamma}{\gamma - 1}}$$

As the length  $l$  and orientation  $\theta$  of each segment of the nozzle contour is known, we can calculate the normal and axial force (per unit depth) by simply resolving the pressure force in the  $x$  and  $y$  direction:

$$F_x = Pl \sin \theta$$

$$F_y = Pl \cos \theta$$

**Table 3 Comparison of integrated forces in  $x$  and  $y$  direction on the upper surface of the nozzle.**

Force Component	MoC	Inviscid CFD	Error	Viscous CFD	Error
$F_x$	-9.303 kN	-9.279 kN	0.26 %	-9.330 kN	0.29 %
$F_y$	40.800 kN	41.288 kN	1.18 %	43.900 kN	7.06 %

Table 3 compares the normal and axial forces acting on the upper surface of the nozzle obtained from MoC with that obtained from inviscid and viscous CFD. Clearly the MoC results are in excellent agreement with inviscid CFD. However, the normal force value obtained from viscous CFD simulation is larger than that obtained from MoC by 7%. This is possibly due to the velocity decrease caused by viscosity in the boundary layer, which would in-turn lead to pressure rise and hence greater pressure force. Nevertheless, as shown in Table 2, the code requires  $< 5s$  for obtaining the nozzle contour with 1000 characteristic lines, and thus, it can serve as a good tool for preliminary design of SERN for scramjets.

## VI. Conclusion

The MoC code developed has a quick run-time of less than 5 seconds for 1000 characteristic lines. The axial and normal forces computed by the MoC code are in excellent agreement with inviscid CFD, but the normal force shows 7% deviation from the viscous CFD simulation. Nevertheless, the code is quasi-1D in nature and can thus be used as a first step for SERN design for scramjets.

## References

- [1] Anderson, J. D., *Fundamentals of aerodynamics*, McGraw-Hill, 2011. URL <http://www.worldcat.org/isbn/9780073398105>.